

## Supramolecular Control of Valence-Tautomeric Equilibrium on Nanometer-Scale Gold Clusters

Sofi Bin-Salamon, Scott Brewer, Stefan Franzen,\* Daniel L. Feldheim,\* Simon Lappi, and David A. Shultz\*

Department of Chemistry, North Carolina State University, Box 8204, Dabney Hall, Yarborough Street, Raleigh, North Carolina 27695-8204

Received December 13, 2004; E-mail: david\_shultz@ncsu.edu; daniel\_feldheim@ncsu.edu; stefan\_franzen@ncsu.edu

Certain metal semiquinone complexes undergo a combined intramolecular electron transfer and spin-crossover called valence tautomerism.<sup>1–3</sup> Cobalt bis(dioxolene)<sup>4</sup> valence tautomers interconvert between an *ls*-Co<sup>III</sup> form with one unpaired electron on a semiquinone (SQ) ligand (*S* = 1/2; Cat = diamagnetic catecholate; bpy = 2,2'-bipyridine) to an *hs*-Co<sup>II</sup> system with two unpaired electrons on the SQ ligands and three unpaired electrons on *hs*-Co<sup>II</sup>, as shown in Scheme 1. The driving force behind valence-tautomeric equilibria lies in the large  $\Delta S^\circ$  and small  $\Delta H^\circ$ . As a consequence,  $\Delta G^\circ$  changes sign as a function of temperature due to the  $T\Delta S^\circ$  contribution to the free energy.

As paramagnetic bistable molecules, valence tautomers are candidates for a variety of molecular switches.<sup>5–7</sup> The feasibility of valence-tautomeric complexes as components of molecular spintronic devices<sup>8,9</sup> is directly related to successful assembly of addressable arrays and control of the switching process. As an initial step in this research area, we show how surface confinement dramatically alters  $\Delta H^\circ$  and  $\Delta S^\circ$  of a valence tautomerism.

Assembling valence-tautomeric complexes onto metal nanoparticle surfaces provides the advantages of solution-phase synthesis and characterization (see Supporting Information) and yields sufficient material to cast high optical density films. Along these lines, we prepared **1**, which is the surface-bound analogue of **2** as shown in Scheme 2. The synthesis of **1** involved generating ca. 2-nm-diameter gold clusters<sup>10</sup> with surface-bound 1-mercapto-6-(4'-methyl)bipyridine.<sup>11</sup> This cluster served as the precursor to generate the final complex by reaction with Co<sub>4</sub>(3,5-(*t*-Bu)<sub>2</sub>C<sub>6</sub>H<sub>2</sub>O<sub>8</sub>)<sub>8</sub>.<sup>12</sup>

Films prepared by evaporation of methylene chloride solutions of **1** and **2** were studied using variable-temperature infrared spectroscopy from 20 to 440 K, and singular value decomposition (SVD)<sup>13</sup> analysis of the vibrational modes was performed. The data were used to construct a profile of the mole fraction of the Co<sup>II</sup> form in the usual way.<sup>2,14</sup> The analysis of the data shown in Figure 1A yielded two SVD components shown in Figure 1B,C.

The first component represents the low temperature (*ls*-Co<sup>III</sup> form) spectrum in the U matrix (wavenumber dimension) and a relatively constant term in the V matrix (temperature dimension). The second component represents the difference between the *ls*-Co<sup>III</sup> and *hs*-Co<sup>II</sup> forms in the wavenumber dimension (Figure 1B). The familiar sigmoidal shape expected from a two-state equilibrium is observed for the temperature dimension of this component (Figure 1D). The sigmoidal curve in Figure 1D was least-squares fit to obtain the thermodynamic parameters as well as  $T_{1/2}$  for the *ls*-Co<sup>III</sup> to *hs*-Co<sup>II</sup> conversion. In addition, we examined model compound **2**.<sup>15</sup> The thermodynamic parameters from our curve fit for **2** are given in Table 1 for comparison to those of **1**.

Our results show that the surface-bound complex possesses a notably different  $T_{1/2}$ ,  $\Delta S^\circ$ , and  $\Delta H^\circ$  compared to the model compound (Table 1). The striking difference between the surface-bound complex and the model compound could be attributed to a

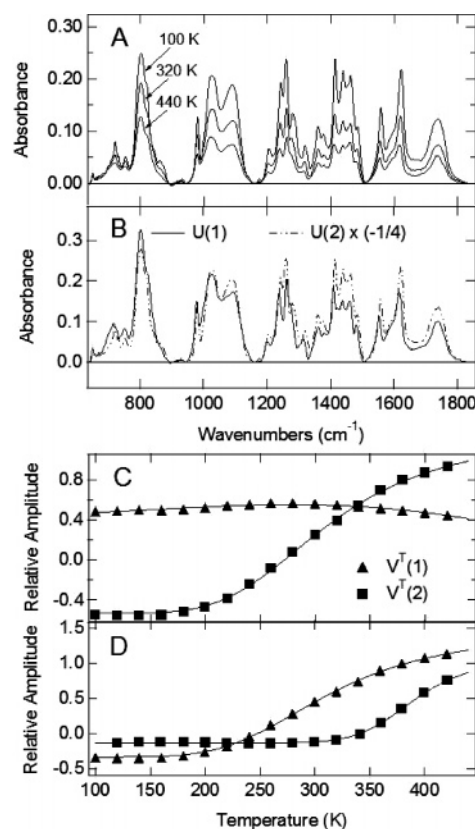
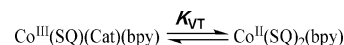
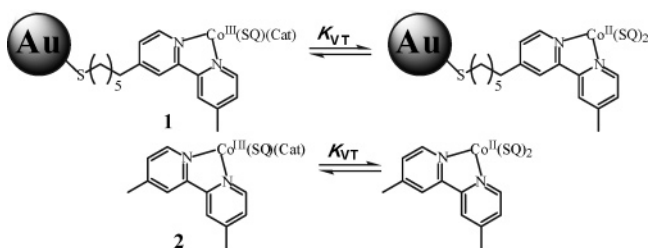


**Figure 1.** (A) Temperature-dependent FTIR spectra of **1** on ca. 2-nm gold nanoparticles in the 100–440 K temperature range recorded in approximately 20 K increments. The first (solid) and second (dashed) spectral components of **1** (B) and the corresponding temperature dependence (C) of the first ( $\blacktriangle$ ) and second ( $\blacksquare$ ) components. (D) The temperature profiles of **1** ( $\blacktriangle$ ) and **2** ( $\blacksquare$ ) of the second spectral components determined by SVD fit to eq 6 (solid curve; see Supporting Information).

## Scheme 1



## Scheme 2



number of possibilities, including surface-charge effects,<sup>16</sup> electronic coupling, spin/vibrational effects, and solvation. The similarity of the vibrational spectra of **1** and **2** (see Supporting Information)

**Table 1.** Thermodynamic Parameters for Valence Tautomerism of **1** and **2**

| parameter                  | 1    | 2    |
|----------------------------|------|------|
| $T_{1/2}$ (K)              | 318  | 389  |
| $\Delta H^\circ$ (kJ/mol)  | 14.3 | 47.5 |
| $\Delta S^\circ$ (J/mol/K) | 44.9 | 122  |

precludes consideration of the gold nanoparticle as a conducting sphere that has well-defined surface selection rules. If the typical metallic surface selection rules were operative, we would expect significant differences in the vibrational spectra of **1** and **2**. Absorption spectra of aromatic dyes exhibit diminished intensity on gold nanoparticles.<sup>17</sup> However, these reported changes in spectral features are inconsistent with the differences in  $\Delta H^\circ$  and  $\Delta S^\circ$  between **1** and **2**. While electronic coupling clearly plays an important role in altering the electronic properties of the adsorbed chromophore, it cannot strongly affect the *entropy* as would be required to account for the changes observed in the thermodynamic parameters. Thus, we rule out both surface charge effects and electronic coupling as major contributors to the large thermodynamic differences observed here.

We are left to consider other possibilities, including spin/vibrational effects and solvation. These contributions to the free energy are:

$$\Delta G^\circ = \Delta G^\circ(\text{spin}) + \Delta G^\circ(\text{vibration}) + \Delta G^\circ(\text{solvation})$$

Since it is widely accepted that the equilibrium is driven largely by the entropic contributions, we focus our discourse on  $\Delta S^\circ$ . The spin contribution is  $\Delta S^\circ(\text{spin}) = R \ln(16/4) = 11.5 \text{ J K}^{-1} \text{ mol}^{-1}$ , and it can be excluded as a major contribution to the overall entropy.<sup>2</sup> It has been proposed that the largest contribution to  $\Delta S^\circ$  arises from changes in metal–ligand bond-stretching frequencies as the valence tautomer interconverts between the *ls*-Co<sup>III</sup> and *hs*-Co<sup>II</sup> forms.<sup>15</sup> This is because of the occupation of  $d\sigma^*$  orbitals in the *hs*-Co<sup>II</sup> form and the resultant lower metal–ligand vibrational frequencies. These low energy modes provide for greater vibrational entropy in the *hs*-Co<sup>II</sup> form by analogy with Fe<sup>II</sup> spin-crossover complexes.<sup>18,19</sup> By this analogy,  $\Delta S^\circ(\text{vibration})$  from previous studies ( $\sim 50\text{--}80 \text{ J K}^{-1} \text{ mol}^{-1}$ )<sup>2</sup> has been assumed reasonable. However, doubt has been cast on the magnitude of  $\Delta S^\circ(\text{vibration})$  by heat capacity measurements reported by Abakumov<sup>20</sup> and by computational results reported by Cox.<sup>21</sup> In addition, Dei et al. have shown that CH<sub>2</sub>Cl<sub>2</sub> solvates behave differently than CD<sub>2</sub>Cl<sub>2</sub> solvates.<sup>22</sup> These findings suggest that  $\Delta S^\circ(\text{solvation})$  might be more important than previously thought.

Since we are dealing with evaporated films that lack vibrational bands for the solvent from which the films were prepared,<sup>14</sup> the valence tautomers themselves act as the solvation sphere. By anchoring the valence tautomer on a metal cluster surface, we have effectively eliminated a large number of intervalence tautomer interaction that arises from the solvation sphere, thereby reducing both  $\Delta H^\circ$  and  $\Delta S^\circ$ .

In conclusion, we synthesized a valence tautomer anchored to a nanometer-scale gold cluster, and we showed that surface attachment attenuates both  $\Delta H^\circ$  and  $\Delta S^\circ$  for the valence tautomerism. We hypothesize that the thermodynamic parameters have changed due to a smaller solvent accessible area caused by surface confinement. Thus, surface confinement itself can be used to “tune” valence tautomerism.

**Acknowledgment.** D.A.S. acknowledges the National Science Foundation (CHE-0345263) for financial support and the Camille and Henry Dreyfus Foundation for a Camille Dreyfus Teacher-Scholar Award. D.L.F. thanks the National Science Foundation (DMR-0303746) for financial support. S.F. gratefully acknowledges support by NSF Grant CHE-0436467.

**Supporting Information Available:** Experimental details, spectra, and equations. This material is available free of charge via the Internet at <http://pubs.acs.org>.

## References

- (1) Pierpont, C. G. *Coord. Chem. Rev.* **2001**, 216, 99–125.
- (2) Shultz, D. A. Valence Tautomerism in Dioxolene Complexes of Cobalt. In *Magnetism: Molecules to Materials II: Molecule-Based Materials*; Miller, J. S., Drillon, M., Eds.; Wiley-VCH: New York, 2001; pp 281–306.
- (3) Gütllich, P.; Dei, A. *Angew. Chem., Int. Ed. Engl.* **1997**, 37, 22734–2736.
- (4) In this communication, “dioxolene” refers to either 3,5-di-*tert*-butyl-1,2-benzosemiquinonate (SQ) or 3,5-di-*tert*-butyl-1,2-catecholate (Cat).
- (5) Carbonera, C.; Dei, A.; Letard, J. F.; Sangregorio, C.; Sorace, L. *Angew. Chem., Int. Ed.* **2004**, 43, 3136–3138.
- (6) Sato, O.; Hayami, S.; Gu, Z.; Seki, K.; Nakajima, R.; Fujishima, A. *Chem. Lett.* **2001**, 874–875.
- (7) Jung, O.-S.; Jo, D. H.; Lee, Y.-L.; Conklin, B. J.; Pierpont, C. G. *Inorg. Chem.* **1997**, 37, 19–24.
- (8) Liang, W.; Shores, M. P.; Bockrath, M.; Long, J. R.; Park, H. *Nature* **2002**, 417, 725–729.
- (9) Wolf, S. A.; Awschalom, D. D.; Buhrman, R. A.; Daughton, J. M.; von Molnar, S.; Roukes, M. L.; Chitcheikanova, A. Y.; Treger, D. M. *Science* **2001**, 294, 1488–1495.
- (10) Brust, M.; Bethell, D.; Schiffrin, D. J.; Kiely, C. J. *Adv. Mater.* **1995**, 7, 795–797.
- (11) Sato, Y.; Uosaki, K. *J. Electroanal. Chem.* **1995**, 384, 57–66.
- (12) Pierpont, C. G.; Buchanan, R. M.; Fitzgerald, B. J. *Inorg. Chem.* **1979**, 18, 3439–3444.
- (13) Vetterling, W. T.; Flannery, B. P. *Numerical Recipes in C++: The Art of Scientific Computing*; Cambridge University Press: New York, 2002.
- (14) See Supporting Information.
- (15) Adams, D. M.; Dei, A.; Rheingold, A. L.; Hendrickson, D. N. *J. Am. Chem. Soc.* **1993**, 115, 8221–8229.
- (16) Moskovits, M.; Suh, J. S. *J. Phys. Chem.* **1984**, 88, 5526–5530.
- (17) Franzen, S.; Folmer, J. C. W.; Glomm, W. R.; O’Neal, R. J. *Phys. Chem. A* **2002**, 106, 6533–6540. The present result indicates that the earlier observations may be due to electronic coupling between the d-band of the nanoparticle and the surface-adsorbed molecule.
- (18) Gütllich, P. *Struct. Bonding (Berlin)* **1981**, 44, 83–195.
- (19) Gütllich, P.; Hauser, A.; Spiering, H. *Angew. Chem., Int. Ed. Engl.* **1994**, 33, 2024–2054.
- (20) Abakumov, G. A.; Cherkasov, V. K.; Bubnov, M. P.; Ellert, O. G.; Dobrokhotova, Z. V.; Zakharov, L. N.; Struchkov, Y. T. *Dokl. Akad. Nauk* **1993**, 328, 332–335.
- (21) LaBute, M. X.; Kulkarni, R. V.; Endres, R. G.; Cox, D. L. *J. Chem. Phys.* **2002**, 116, 3681–3689.
- (22) Cador, O.; Dei, A.; Sangregorio, C. *Chem. Commun.* **2004**, 652–653.

JA042520Q